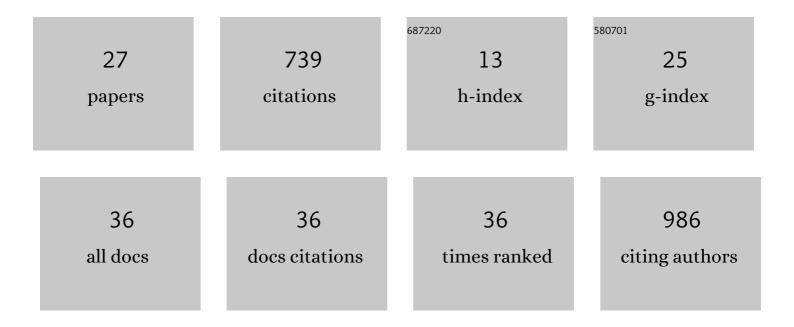
Wolf Achim Kahl

List of Publications by Year in descending order

Source: https://exaly.com/author-pdf/8780951/publications.pdf Version: 2024-02-01



#	Article	IF	CITATIONS
1	Morphological transition during prograde olivine growth formed by high-pressure dehydration of antigorite-serpentinite to chlorite-harzburgite in a subduction setting. Lithos, 2021, 382-383, 105949.	0.6	4
2	Hydrothermal troctolite alteration at 300 and 400°C – Insights from flexible Au-reaction cell batch experimental investigations. American Mineralogist, 2021, , .	0.9	0
3	Variant across-forearc compositions of slab-fluids recorded by serpentinites: Implications on the mobilization of FMEs from an active subduction zone (Mariana forearc). Lithos, 2020, 364-365, 105525.	0.6	9
4	Ambient occlusion – A powerful algorithm to segment shell and skeletal intrapores in computed tomography data. Computers and Geosciences, 2018, 115, 75-87.	2.0	11
5	Textural evolution during high-pressure dehydration of serpentinite to peridotite and its relation to stress orientations and kinematics of subducting slabs: Insights from the Almirez ultramafic massif. Lithos, 2018, 320-321, 470-489.	0.6	18
6	3â€D microstructure of olivine in complex geological materials reconstructed by correlative Xâ€ray T and EBSD analyses. Journal of Microscopy, 2017, 268, 193-207.	0.8	15
7	Reaction-induced porosity and onset of low-temperature carbonation in abyssal peridotites: Insights from 3D high-resolution microtomography. Lithos, 2017, 268-271, 274-284.	0.6	23
8	Classical and new bioerosion trace fossils in Cretaceous belemnite guards characterised via micro-CT. Fossil Record, 2017, 20, 173-199.	0.5	17
9	A new X-ray-transparent flow-through reaction cell for a <i>î¼</i> -CT-based concomitant surveillance of the reaction progress of hydrothermal mineral–fluid interactions. Solid Earth, 2016, 7, 651-658.	1.2	5
10	Lightweight aggregates from mixtures of granite wastes with clay. Journal of Cleaner Production, 2016, 117, 139-149.	4.6	47
11	Experimental constraints on fluid-rock reactions during incipient serpentinization of harzburgite. American Mineralogist, 2015, 100, 991-1002.	0.9	66
12	Ultramafic clasts from the South Chamorro serpentine mud volcano reveal a polyphase serpentinization history of the Mariana forearc mantle. Lithos, 2015, 227, 1-20.	0.6	31
13	Magnetite in seafloor serpentiniteSome like it hot. Geology, 2014, 42, 135-138.	2.0	192
14	Traces of the bone-eating annelid Osedax in Oligocene whale teeth and fish bones. Palaontologische Zeitschrift, 2013, 87, 161-167.	0.8	24
15	Microfabric and anisotropy of elastic waves in sandstone – An observation using high-resolution X-ray microtomography. Journal of Structural Geology, 2013, 49, 35-49.	1.0	13
16	Microstructure and reactivity of calcined mud supported limestones. Institutions of Mining and Metallurgy Transactions Section C: Mineral Processing and Extractive Metallurgy, 2012, 121, 5-11.	0.6	7
17	Non-destructive fabric analysis of prehistoric pottery using high-resolution X-ray microtomography: a pilot study on the late Mesolithic to Neolithic site Hamburg-Boberg. Journal of Archaeological Science, 2012, 39, 2206-2219.	1.2	58
18	Thermodynamic properties of scorodite and parascorodite (FeAsO4·2H2O), kaÅ^kite (FeAsO4·3.5H2O), and FeAsO4. Hydrometallurgy, 2012, 117-118, 47-56.	1.8	62

Wolf Achim Kahl

#	Article	IF	CITATIONS
19	Thermal microstructural changes of grain-supported limestones. Mineralogy and Petrology, 2011, 103, 9-17.	0.4	8
20	Osedax borings in fossil marine bird bones. Die Naturwissenschaften, 2011, 98, 51-55.	0.6	30
21	Fossil traces of the bone-eating worm <i>Osedax</i> in early Oligocene whale bones. Proceedings of the United States of America, 2010, 107, 8656-8659.	3.3	54
22	Thermodynamic properties of magnesiochloritoid. European Journal of Mineralogy, 2005, 17, 587-598.	0.4	5
23	Enthalpy of formation of pargasite by high-temperature solution calorimetry and heat capacity of pargasite and fluoropargasite by differential scanning calorimetry. European Journal of Mineralogy, 2003, 15, 617-628.	0.4	6
24	Thermodynamic data of the high-pressure phase Mg 5 Al 5 Si 6 O 21 (OH) 7 (Mg-sursassite). Physics and Chemistry of Minerals, 2001, 28, 475-487.	0.3	14
25	Enthalpies of formation of tremolite and talc by high-temperature solution calorimetry—a consistent picture. American Mineralogist, 2001, 86, 1345-1357.	0.9	13
26	Multiple pyroxene and amphibole assemblages in the amphibolite facies: Bulk compositional controls. American Mineralogist, 2000, 85, 1606-1616.	0.9	4
27	Design of the subsurface observatory at Surtsey volcano, Iceland. Scientific Drilling, 0, 25, 57-62.	1.0	3